

## Swelling properties and basic dye adsorption studies of polyacrylamide hydrogel

Imane Lebkiri<sup>a,\*</sup>, Brahim Abbou<sup>a</sup>, Lamyia Kadiri<sup>a</sup>, Abdelkarim Ouass<sup>a</sup>,  
Abdelhay Elamri<sup>a</sup>, Hanae Ouaddari<sup>b</sup>, Omar Elkhattabi<sup>a</sup>, Ahmed Lebkiri<sup>a</sup>,  
El Houssein Rifi<sup>a</sup>

<sup>a</sup>Laboratory of Advanced Materials and Process Engineering, Faculty of Sciences, Ibn Tofail University, Kenitra, Morocco, emails: imane.lebkiri@gmail.com (I. Lebkiri), abbou.brahim@gmail.com (B. Abbou), kadiri.lamyia@gmail.com (L. Kadiri), karim.ouass.smp@gmail.com (A. Ouass), elamriabdelhay@gmail.com (A. Elamri), omarkhatt@gmail.com (O. Elkhattabi), lebkiriahm@yahoo.fr (A. Lebkiri), elhosseinr@yahoo.fr (E.H. Rifi)

<sup>b</sup>Laboratory of Materials Membranes and Environment, Department of Chemistry, Faculty of Sciences and Technologies of Mohammedia, University of Hassan II, Casablanca, Morocco, email: ouaddarihanae@gmail.com

Received 14 February 2021; Accepted 16 June 2021

---

### ABSTRACT

This study regrouped the swelling of polyacrylamide (PAAM) hydrogel and the use of this hydrogel in the removal of Safranin (SF) basic dye from an aqueous solution. The swelling experiments results show that the swell ratio of this hydrogel depends on several parameters: the presence of salts, the temperature, and the pH of the medium. Indeed, in the presence of distilled water only the polymer is capable of retaining its macromolecular chains more than 100 times its weight in water. On the other hand, the adsorption process of SF dye by PAAM polymer was investigated using independent variables namely initial pH, dye ion concentration, temperature, and adsorbent dosage. SF adsorption capacity of PAAM hydrogel is found to be 620 mg/g and the equilibrium is obtained after 3 h. The adsorption process could be well described by the Langmuir isotherm and pseudo-first-order model in both linear and non-linear regressions. The adsorption was analyzed thermodynamically and the results revealed that the adsorption process was spontaneous and endothermic.

*Keywords:* Polyacrylamide; Swelling; Hydrogel; Adsorption; Safranin; Basic dye

---

### 1. Introduction

Great interest has been growing in the synthesis and various applications of superabsorbent hydrogels [1,2]. Hydrogels, a novel functional polymer material with a three-dimensional network structure, are moderately cross-linked hydrophilic network polymers that can quickly swell in water and conserve it to a certain degree in comparison with general similar materials like cloth, cotton and cellulose fiber, and so forth [3]. Polymeric hydrogels have also

generated great interest because of their sensitivity to environmental stimuli such as temperature, pH, pressure, and ionic strength [4,5]. So far, they were extensively used in a variety of application areas such as separation membranes, biosensors, artificial muscles, superabsorbents, such as hygienic products, as well as waste-water treatment and drug delivery devices in virtue of their low cost, abundant resources, and biodegradability [6,7].

Recently, the continuous growth of the world's water population has gained much attention and dyes are major

---

\* Corresponding author.

water pollutants [8]. Dyes are widely used in the textile, leather, paper, pharmaceutical, plastic, and food industries. The extensive use of dyes often causes pollution problems and endangers the equilibrium of the natural ecosystem when they are discarded into wastewater [9,10]. The genotoxic and mutagenic agents of dyes are more problematic because they can cause heritable disorders that may pass to future generations [11]. Therefore, it is necessary to monitor the environment for quality assurance [12].

Many processes such as biological treatment, coagulation, flotation, electrochemical techniques, adsorption, and oxidation are used to remove dyes from wastewater [13,14]. Adsorption has been the most preferred technique for dye wastewater treatment in terms of cost, simplicity of design, ease of operation, and insensitivity to toxic substances [15,16]. Polymeric hydrogels such as polyacrylamide gel have been the focus of research for environmental scientists due to their characteristic properties, namely adsorption-regeneration, economic feasibility, and environmentally friendly behavior [17,18].

Polyacrylamide hydrogel is a functionalized polymer containing a large number of amide groups which grant a great selectivity for the elimination of several organic pollutants and minerals [19]. Due to its low cost, recoverability, biodegradability, high-adsorption capacity, and its use without any modification, PAAM can be a great adsorbent for dye removal from wastewater [20,21]. Moreover, one of the important advantages of using this polymer is its structure containing abundant active sites which makes it capable of fixing dyes species. Also, the shape and the mechanical rigidity of the adsorbent promote the separation procedure at the end of the adsorption experience.

According to our knowledge, there is no report in the literature about the use of polyacrylamide hydrogel in the adsorption of Safranin (SF) dye. There are only a few studies that have reported the use of this hydrogel in dyes removals, such as the removal of methyl violet from aqueous solution by polyacrylamide by Rahchamani et al. [22], the removal of anionic dyes (reactive orange-20 and direct red-31) from aqueous solutions using polyacrylamide by Didehban et al. [23] and application of polyacrylamide for methylene blue removal from aqueous solutions by Mousavi et al. [24].

### 1.1. Aims and objectives

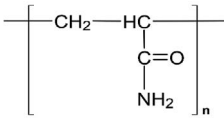
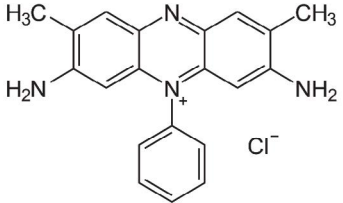
This present study aims to investigate the swelling of PAAM hydrogel in a solution with varied ionic strength, pH, and temperature. We further studied the adsorption abilities, kinetics, and isotherms of SF basic dye by the polyacrylamide polymer from aqueous solutions.

## 2. Experimental section

### 2.1. Studied materials

The material used in this work is polyacrylamide (PAAM) whose chemical formula is  $([-C_2H_3CONH_2-])_n$  (Table 1). It is a superabsorbent that has the form of transparent beads of non-porous surface aspect supplied by Sigma-Aldrich (Saint Louis, USA), (CAS number: 9003-05-8, purity: 99.99%, MW: 150,000).

Table 1  
Structure of polyacrylamide polymer and Safranin dye

The polyacrylamide polymer structure	Safranin dye structure
	

The dye used in this work is SF, a cationic dye supplied by SOLVACHIM (Casablanca, Morocco). Its chemical formula is  $C_{20}H_{19}N_4^+Cl^-$  (M.W. = 350.84 g mol<sup>-1</sup>,  $\lambda_{max}$  = 519 nm, purity: 85%), and its structure is given in Table 1. SF stock solution with an initial concentration of 1,000 mg L<sup>-1</sup> was prepared by dissolving the required amount in double-distilled water. The test solutions were prepared by diluting the stock solution to the desired concentrations.

Other reagents like hydroxide sodium ( $\geq 97.0\%$ ), sodium nitrate (99%), potassium chloride (99%), sodium chloride (99%), and hydrochloric acid (37%) are supplied by Sigma-Aldrich (Saint Louis, USA).

### 2.2. Measurement of the swelling rate

A dry amount of PAAM polymer ( $m_s$ ) was immersed in a given volume of distilled water at 25°C with stirring. When the maximum swelling rate is reached the resulting gel has been weighed ( $m_g$ ). The swelling rate (Sr) is determined using the following equation:

$$Sr = \frac{m_g}{m_s} \quad (1)$$

The water absorbed by PAAM hydrogels is quantitatively represented by the equilibrium water content (EWC):

$$EWC = \frac{m_g - m_s}{m_g} \quad (2)$$

### 2.3. Adsorption experiments

The adsorption experiments were carried out in a static regime in a stirred reactor at a fixed temperature (25°C  $\pm$  2°C). The quantities of dye adsorbed and the dye removal efficiency were calculated from the concentrations of the solutions, before and after adsorption according to the following equations [25,26]:

$$Q = \frac{C_i - C_f}{m} \times V \quad (3)$$

$$R\% = \frac{(C_i - C_f)}{C_i} \times 100 \quad (4)$$

where  $Q$  is the adsorbed capacity of PAAM at equilibrium (mg/g),  $R\%$  is the dye removal efficiency (%),  $C_i$  and  $C_f$  are, respectively, the initial and the equilibrium dye concentration (mg/L),  $m$  is the mass of adsorbent (g) and  $V$  is the volume of the dye solution (mL).

The SF dye content analyzes were carried out at room temperature using a UV-Visible spectrophotometer (Perkin Elmer Lambda 35).

All tests were repeated three times and the average values were used. For quality assurance/quality control (QA/QC), Sf concentrations in all tests were measured separately and the error percentage was less than 3%.

2.3.1. Method validation

The analytical method developed herein was validated by determining its linearity, limit of detection and quantification (LOD, LOQ). Linearity was studied based on the external standard method and the concentrations of cationic dye were 1, 2, 4, 6, 8, 10 mg/L. The best fit standard curve was prepared by linear regression and the correlation coefficient obtained was more than 0.999 (Table 2).

The LOD, LOQ values were intended using standard equations [27]:

$$\text{LOD} = 3 \cdot \frac{S}{m} \quad \text{and} \quad \text{LOQ} = 10 \cdot \frac{S}{m} \tag{5}$$

where  $S$  is the standard deviation of slope and  $m$  is the slope of calibration curve.

The LOD, LOQ values were calculated as 0.035 and 0.0106 mg/L, respectively (Table 2). According to the current results with good sensitivity and lower detection limit suggests that the method is better compared to other methods reported.

2.4. Model to experimental data

- Adsorption kinetics analysis was calculated using [28,29]: The pseudo-second-order rate equation as:

$$\frac{dQ_t}{dt} = K_2(Q_e - Q_t)^2 \Leftrightarrow \frac{t}{Q_t} = \frac{1}{K_2 Q_e^2} + \frac{1}{Q_e} t \tag{6}$$

The pseudo-first-order rate equation as:

$$\frac{dQ_t}{dt} = K_1(Q_e - Q_t) \Leftrightarrow \ln(Q_e - Q_t) = \ln Q_e - K_1 t \tag{7}$$

where  $K_1$  is the pseudo-first-order rate constant (g/mg min);  $K_2$  is the pseudo-second-order rate constant (g/mg min),  $Q_e$  and  $Q_t$  are the metal uptake (mg/g) at equilibrium and at time  $t$ , respectively.

- The Freundlich and Langmuir sorption isotherm equations are given respectively below [30,31]:

$$Q_e = K_f C_e^{\frac{1}{n}} \Leftrightarrow \log(Q_e) = \log(K_f) + \frac{1}{n} \log(C_e) \tag{8}$$

$$Q_e = Q_m \frac{K_L C_e}{1 + K_L C_e} \Leftrightarrow \frac{C_e}{Q_e} = \frac{1}{K_L Q_m} + \frac{C_e}{Q_m} \tag{9}$$

where  $K_f$  is the Freundlich isotherm constant (mg/g),  $n$  is the adsorption intensity,  $C_e$  is the equilibrium concentration of adsorbate (mg/L);  $Q_e$  is the adsorption capacity at equilibrium (mg/g),  $Q_m$  is the maximum monolayer coverage capacity (mg/g) and  $K_L$  is the Langmuir isotherm constant (L/mg).

The separation factor ( $R_L$ ) was used to determine whether the adsorption was favorable or not. The  $R_L$  was calculated from the following equation [32]:

$$R_L = \frac{1}{1 + K_L C_0} \tag{10}$$

where  $C_0$  represents the initial concentration of adsorbate (mg/L).

- For the thermodynamic studies, the Eyring equation was used [33]:

$$\ln K = \left( \frac{\Delta S}{R} \right) - \left( \frac{\Delta H}{R} \right) \frac{1}{T} \tag{11}$$

where  $K$  is the sorption distribution constant ( $K = Q_e/C_e$ ),  $R$  is the ideal gas constant (8,314 J mol<sup>-1</sup> K<sup>-1</sup>) and  $T$  is the temperature (K),  $\Delta G$  is the Gibbs free energy (J/mol),  $\Delta S$  is the entropy (J/k mol) and  $\Delta H$  is the enthalpy (J/mol).

2.5. Error function analysis

In order to evaluate the suitability of a model equation to experimental results, an error function assessment is usually required [34,35]:

- Coefficient of determination ( $R^2$ ): Its value varies from 0 to 1 and is given as in Eq. (10). It provides the best fitting when its value is closest to unity:

$$R^2 = 1 - \frac{\sum(Q_{e,exp} - Q_{e,calc})^2}{\sum(Q_{e,exp} - Q_{e,mean})^2} \tag{12}$$

- The chi-square ( $\chi^2$ ): A high  $\chi^2$ -value indicates a high bias between the experimental and the calculated model values.

Table 2  
Calibration curve, LOD, and LOQ

Regression equation	Standard deviation		$R^2$	LOD	LOQ
	Slope	Intercept			
$y = 12.948x - 0.8318$	0.07934	0.015146	0.9996	0.03521768	0.10602326

$$\chi^2 = \sum \frac{(Q_{e,\text{exp}} - Q_{e,\text{calc}})^2}{Q_{e,\text{calc}}} \quad (13)$$

- The sum of error squares (SSE): The lower the value, the better the curve fits the experimental values. It is mathematically expressed in Eq. (12).

$$\text{SSE} = \sum (Q_{e,\text{cal}} - Q_{e,\text{exp}})^2 \quad (14)$$

- The standard error (SE):

$$\text{SE} = \sqrt{\text{SSE} / N} \quad (15)$$

with  $N$  is the degrees of freedom.

In addition to the previously mentioned error equations, another statistical test, namely  $F$ -test, is examined for their suitability to be the appropriate function to predict the best-fitting isotherm model.

### 3. Experimental results and discussion

#### 3.1. Characterization of PAAM

##### 3.1.1. Fourier-transform infrared spectroscopy of PAAM

IR spectrometry makes it possible to interpret the spectra obtained by detecting the functional groups of the molecule. The infrared spectra ( $400\text{--}4,000\text{ cm}^{-1}$ ) of PAAM are shown in Fig. 1a. The spectrum shows two peaks at  $3,465.44$  and  $3,405\text{ cm}^{-1}$  due to the valence vibration of the amino group N–H stretching (primary amine) and the hydroxyl group (OH) [36–38]. The absorption peak at  $2,923\text{ cm}^{-1}$  could be attributed to the C–H elongation vibration of the  $\text{CH}_2$  group. The adsorption peak at  $1,639\text{ cm}^{-1}$  confirms the presence of the carboxyl group C=O and that at  $1,382\text{ cm}^{-1}$  corresponds to the valence vibration of C–N, whereas that at  $998\text{ cm}^{-1}$  and  $622\text{ cm}^{-1}$  corresponds to the valence vibration of  $\text{NH}_2$  [39–41].

##### 3.1.2. X-ray diffraction

X-ray diffraction makes it possible to determine the structure of the polymer studied. Fig. 1b shows the X-ray diffraction pattern of the polymer in powder form. The absence of peaks in the spectrum of this figure shows that the polymer studied is an amorphous product [42].

##### 3.1.3. Point of zero charge

The PZC was determined by a simple electrochemical method, by adding  $0.013\text{ g}$  of PAAM in a series of beakers containing  $50\text{ mL}$  of NaCl ( $0.01\text{ M}$ ), the  $\text{pH}_i$  (initial pH) of each beaker was adjusted to precise values from 2 to 12 then  $0.013\text{ g}$  [43]. The suspensions were kept under constant stirring at room temperature for 24 h. At the end of the experiment, the final pH ( $\text{pH}_f$ ) values of the suspensions were recorded. The value of PZC is the intersection of the curve ( $\Delta\text{pH}$  ( $\text{pH}_f - \text{pH}_i$ ) vs.  $\text{pH}_i$ ) with the abscise axis (Fig. 1c). The PZC of PAAM is equal to 8.1. For  $\text{pH} > \text{PZC}$ ,

the surface of the support is negatively charged while for  $\text{pH}$  less than 8.1 the surface is positively charged.

#### 3.2. Swelling of PAAM in distilled water

A mass equal to  $13\text{ mg}$  of PAAM was placed in a beaker containing  $100\text{ mL}$  of distilled water. The gel obtained was weighed at regular time intervals to determine the rate of gel swelling. Fig. 2a shows the evolution of the rate of swelling of the gel versus time. At the beginning of the experiment, significant absorption of water by the polymer is observed. The equilibrium of swelling is reached after the first 7 h  $\text{Sr} = 100$ . The water sorption phenomenon by hydrogel mechanically depends on the diffusion of the water molecules in the gel matrix and, therefore, the expansion of the macromolecular chains of the hydrogel under the osmotic effect [44].

To illustrate this phenomenon, we represented in Fig. 2b, the evolution of the equilibrium water content (EWC) of PAAM versus its residence time in distilled water. The maximum EWC is 0.98. Thus, the value determined here, falls in the same range as previously reported values in literature, for similar hydrogel systems [45,46].

The PAAM bead (after swelling) has a diameter of  $1.5\text{ cm}$ , it exhibits high mechanical strength and can support a  $150\text{ g}$  weight without causing any significant deformation. It is worthy of note that the density of PAAM is extremely low, which is in the range of  $0.08\text{--}0.092\text{ g cm}^{-3}$ .

##### 3.2.1. Swelling behavior in salt solutions

Concentrations of  $\text{NaNO}_3$  and KCl solutions ranging from  $0.01$  to  $1\text{ M}$  were prepared. In each solution, we introduced  $13\text{ mg}$  of PAAM. The swelling rates of the polymer were measured after 7 h of contact at different concentrations of  $\text{NaNO}_3$  and KCl. It can be shown from Fig. 2c that the rate of swelling decreases with the increasing ionic strength of the medium. The main reason for this ionic dependence on swelling is the balance between the osmotic pressure of the swelling system and the elastic response of the polymer which controls the extent of the swelling. The osmotic pressure results from the difference between the concentrations of mobile ions inside the hydrogel network and the external immersion medium [47]. The increase in ionic concentration reduces the difference in concentration of mobile ions between the polymer gel and the external medium (osmotic swelling pressure), which, in turn, reduces the volume of the gel, i.e. as the gel contracts [48].

##### 3.2.2. Influence of pH on the swelling of PAAM

Fig. 2e illustrates the curve representing the effect of pH on the swelling of PAAM. We notice from the curve, at the very acidic pH we get uncharged gels with a low swelling rate  $\text{Sr} = 3.3$ . For pH values above 3, the value of the swelling rate is higher  $\text{Sr} = 103$ . However, at pH values above 8, the swelling rate of the polymer decreases until  $\text{Sr} = 52.34$ . The results can be attributed to the fact that, as the pH of the solution increases, the amide groups of the crosslinked PAAM chains undergo hydrolysis and are

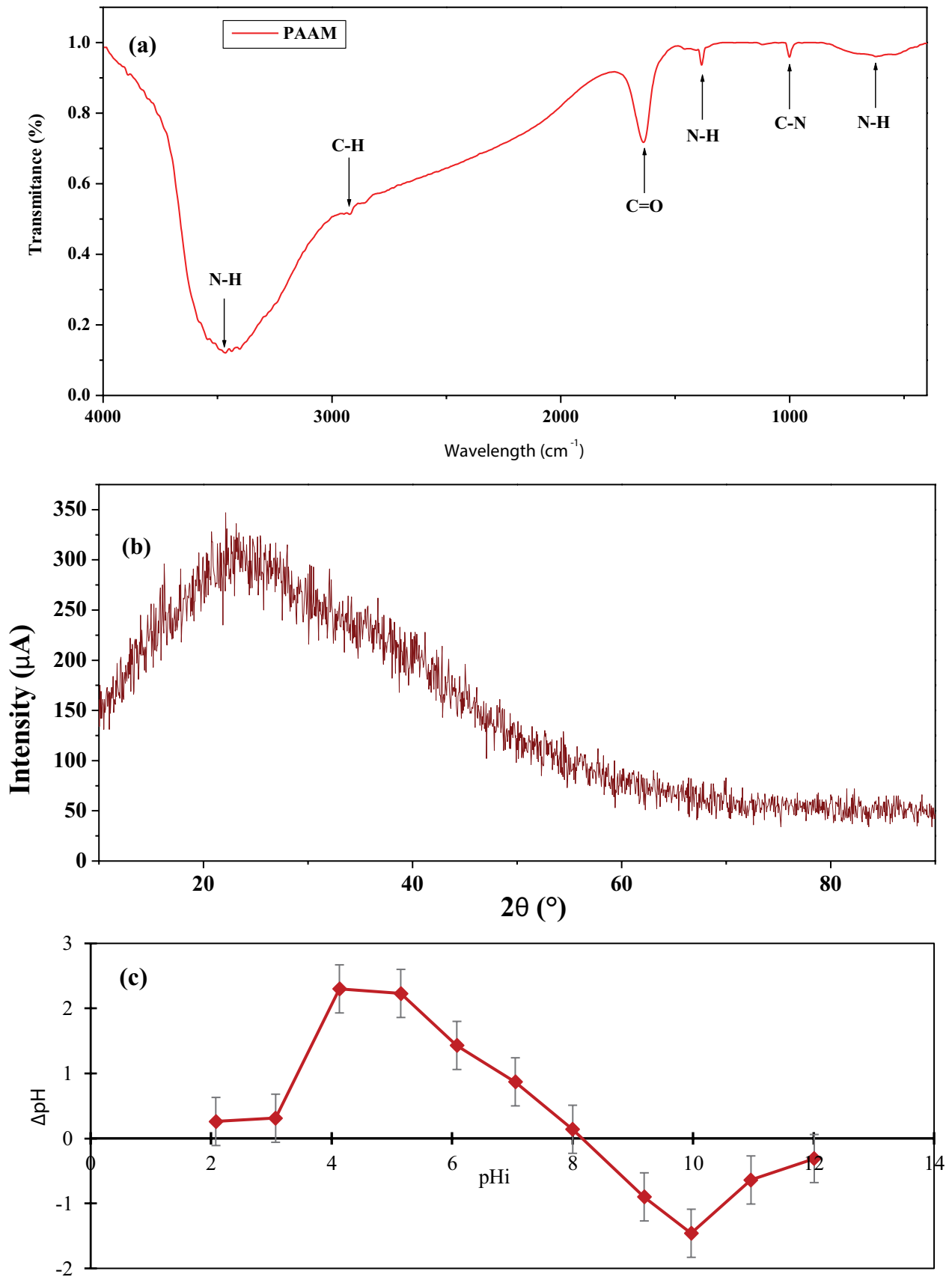


Fig. 1. (a) IR spectrometry of PAAM, (b) X-ray diffraction of PAAM, and (c) Point of zero charge (ZCP).

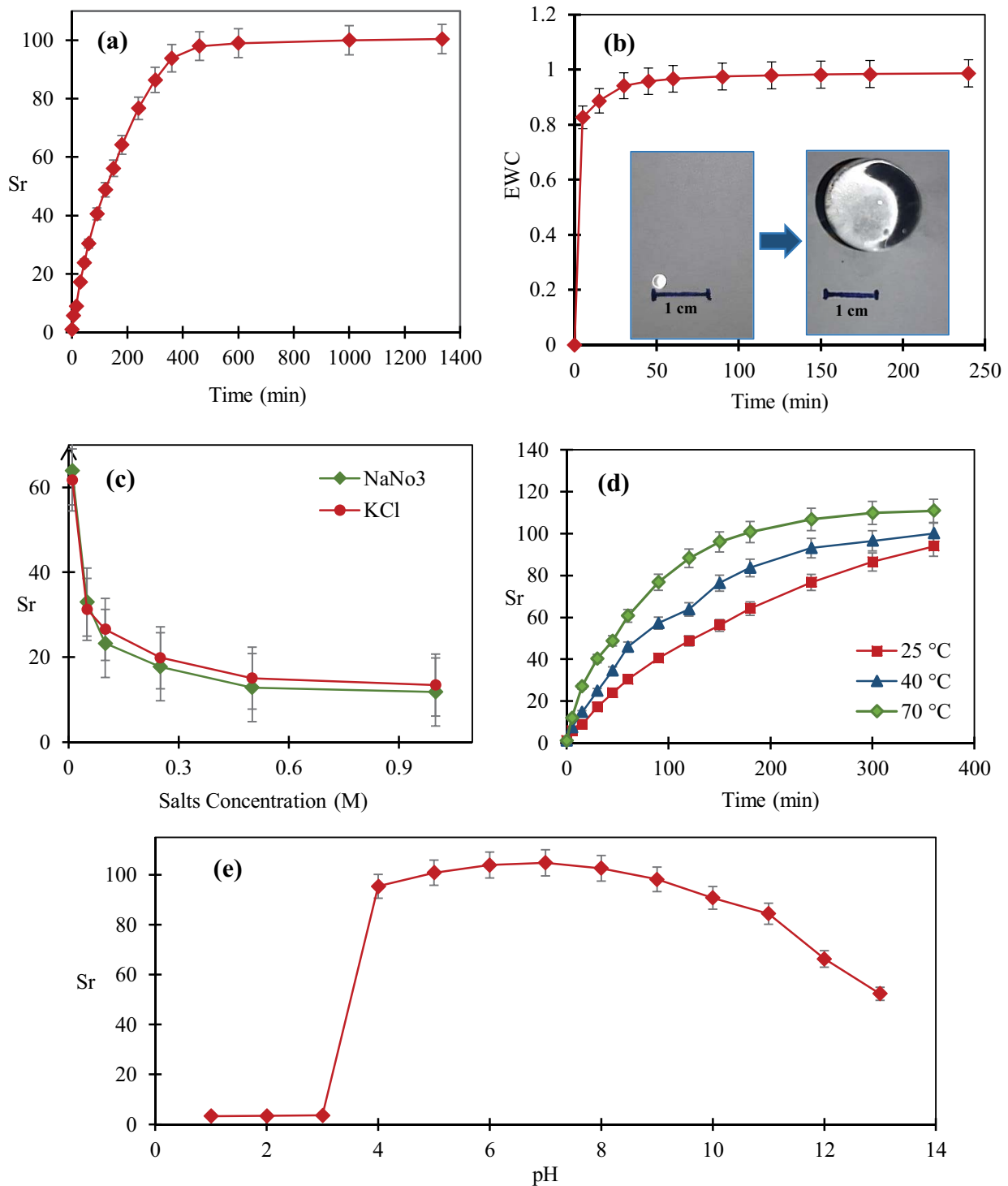


Fig. 2. Evolution of the swelling rate (a) and the EWC (b) of the PAAM in distilled water ( $m = 13$  mg,  $V = 100$  mL,  $T = 25^\circ\text{C}$ ). (c) Effect of concentration of salts on Sr ( $t = 7$  h,  $m = 13$  mg,  $V = 100$  mL,  $T = 25^\circ\text{C}$ ). (d) Temperature effect on Sr ( $t = 6$  h,  $m = 13$  mg,  $V = 100$  mL,  $T = 25^\circ\text{C}$ – $45^\circ\text{C}$ – $75^\circ\text{C}$ ). (e) Influence of the pH on Sr ( $t = 7$  h,  $m = 13$  mg,  $V = 100$  mL,  $\text{pH} = 1$ – $13$ ,  $T = 25^\circ\text{C}$ ).

converted to carboxylic groups which begin to ionize as the pH increases. This produces anionically charged polymer chains which, due to the mutual repulsion between the carboxylate ions, cause the chains of the network to expand, resulting in increased swelling. However, beyond

a certain pH (8.1 in this case), it is observed that the swelling decreases. The reason for the decrease observed may be that, at higher pH, the ionic concentration becomes large in the external medium and, consequently, the swelling decreases [49].

### 3.2.3. Influence of temperature on the swelling of PAAM

To study the effect of temperature on the swelling of PAAM, the experiments were carried out at different temperatures 25°C, 45°C, and 75°C (Fig. 2d). We observe from the curves obtained that the rate of swelling of the gel goes up as the temperature increases,  $S_r$  goes from 93.84 to 110.82 from 25°C to 75°C. Indeed, the increase in temperature can affect the elastic properties of the macromolecular chains, they expand and therefore absorb significant quantities of water. When the temperature increases, the interaction behavior disturbs the disentanglement of interpenetrated polymeric chains and destruction of hydrogen bonding between polymer molecules occurs. Thus, the swelling ratio increases, Tippabattini Jayaramudu et al. found the same result [50].

## 3.3. Safranine dye adsorption studies by PAAM

### 3.3.1. Effect of shaking time

We tracked in time, the adsorption performance of SF dye (10 mg/L) in contact with PAAM (Fig. 3a). This step is essential to know the time at which the gel balances with the dye solution. It is clear that the curve obtained shows two adsorption stages. The first stage shows a sharp increase in the rate of dye removal to almost 90% with increasing the contact time from 0 to 180 min. Above 3 h comes the second stage where the rate is nearly fixed with increasing the contact time from 180 min to 300 min. This stage is representing the equilibrium stage, that is, the equilibrium was obtained after 180 min contact time with a yield of 90%. Such adsorption behavior is common and credited mainly to the almost total occupation of active sites dye ions with increasing the contact time, under our experimental conditions [51]. Fig. 4 illustrates the adsorption of SF dye on PAAM.

## 3.4. Kinetic modeling

The adsorption kinetics represents the evolution of an adsorption process parameter over time. It provides information about the mechanism of adsorption and the mode of transfer of solutes from the liquid phase to the solid phase. Two of the most widely used kinetic models, that is pseudo-first-order and pseudo-second-order equations were used to research the adsorption kinetic behavior of SF onto PAAM polymer (Fig. 5). The parameters of the two kinetic models were estimated by linear and nonlinear regressions. The resulting kinetic parameters and error function data are presented in Table 3.

According to Tables 3 and 4, it seems that the pseudo-first-order model is the most suitable model to satisfactorily describe the studied adsorption phenomenon. Indeed, the highest  $R^2$ -value and the lowest SEE,  $\chi^2$ , SE, and  $F$ -values were found when modeling the equilibrium data using the pseudo-first-order, for both linear and non-linear regression analysis. Also, the calculated value of the adsorbed capacity at the equilibrium of the pseudo-first-order model agrees with the experimental data. These results show that the adsorption process follows the pseudo-first-order model and that nonlinear regression

analysis is the best method to obtain realistic parameters. A similar observation was reported by Moussout et al. [52].

### 3.4.1. Effect of the adsorbent dose

The effect of the increasing adsorbent dose (from 0.007 g to 0.08) on the adsorption rate of SF dye (10 mg/L) was studied (Fig. 3b). The curve shows that the removal efficiency of SF increases rapidly, when the PAAM dose increase from 0.007 g to 0.026 g. It appeared that the use of 0.026 g of PAAM eliminates more than 90% of the SF dye. Beyond 0.026 g, there is no significant change, the elimination rate reaches almost 96% for mass up to 0.065 g of PAAM. This result is due to the fact that as the adsorbent dosage increases, the adsorbent sites available for the dye molecules also increase and consequently better adsorption takes place [53]. Thus, the adsorbent mass was set at 0.026 g (2 beads) for further experiments. Those results are similar to the ones found by Ghezali et al. [54].

### 3.4.2. Effect of the pH

The influence of pH on the adsorption of SF dye (10 mg/L) by PAAM was studied using different values of pH (from 1 to 12) (Fig. 3e). The results indicate that at low pH values (pH < 2), there is no adsorption as there is competition between  $SF^+$  and  $H^+$  protons to bind to the surface of the PAAM polymer, then the adsorption efficiency of the dye increases considerably (89%) as the pH value rises from 2 to 4, then it increases slightly as the pH value rises from 4 to 8 reaching its maximum (95.5%). This is in accordance with the pH range of the wastewater [55,56]. A further increase in the pH value results in a significant decrease in the removal rate of the SF dye this is due to the deflation of the PAAM gel at basic pH as shown in Fig. 8. The same results are obtained in other work [57].

### 3.4.3. Effect of the temperature

The influence of temperature on the adsorption of SF by PAAM gel was also investigated. The experiments were conducted by adding the same amount of PAAM to the SF dye solution at different temperatures (25°C, 35°C, 45°C and 55°C) for 60 min (Fig. 3c). The curve obtained shows that an increase in temperature from 25°C to 55°C is accompanied by an increase in the adsorption efficiency of SF from 52% to 87%. This phenomenon suggests that the reaction is endothermic as the increasing temperature promotes the mechanism of adsorption. It is well known that temperature can affect several aspects of dye adsorption. In fact, the temperature has a positive influence on the increase in the swelling of an adsorbent, the mobility of dye molecules, the number of active sites, and the interaction between adsorbate and adsorbent [58]. Similar findings have also been reported by other researchers as well Liu et al. [59].

## 3.5. Thermodynamic studies

The thermodynamic study provides additional information on inherent energetic changes of the adsorption process of SF dye by PAAM. The thermodynamic parameters

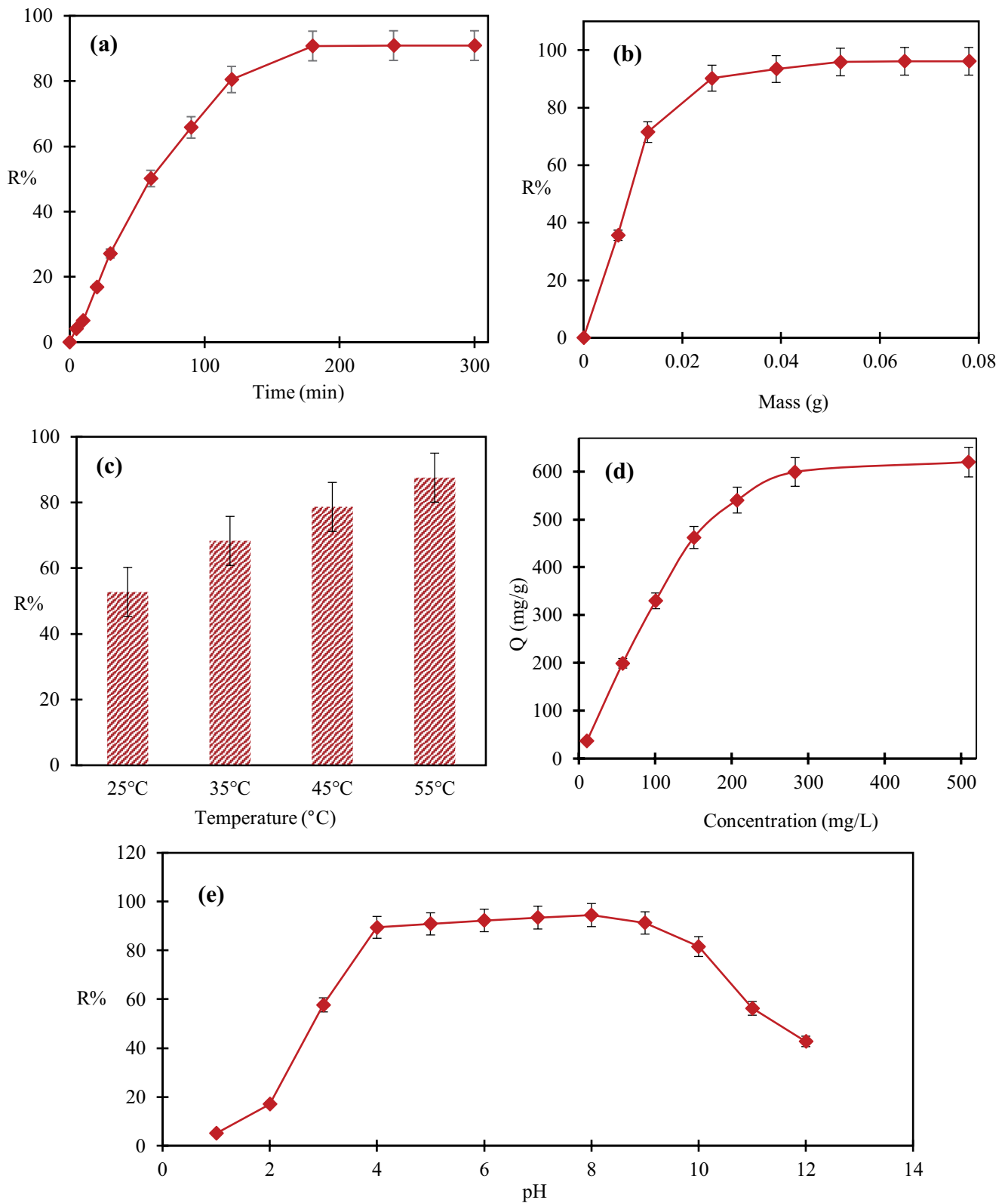


Fig. 3. Adsorption rate of SF by PAAM versus (a) time ( $m = 26$  mg,  $V = 100$  mL,  $[SF] = 10$  mg/L,  $T = 25^\circ\text{C}$ ), (b) PAAM adsorbent dose ( $\text{pH} = 5$ ,  $V = 100$  mL,  $[SF] = 10$  mg/L,  $T = 25^\circ\text{C}$ ), (c) temperature ( $\text{pH} = 5$ ,  $V = 100$  mL,  $[SF] = 10$  mg/L,  $m = 26$  mg), (e) pH ( $m = 26$  mg,  $V = 100$  mL,  $[SF] = 10$  mg/L,  $T = 25^\circ\text{C}$ ). (d) Adsorption capacity versus the initial concentration of SF dye pH ( $m = 26$  mg,  $V = 100$  mL,  $T = 25^\circ\text{C}$ ,  $\text{pH} = 5$ ).



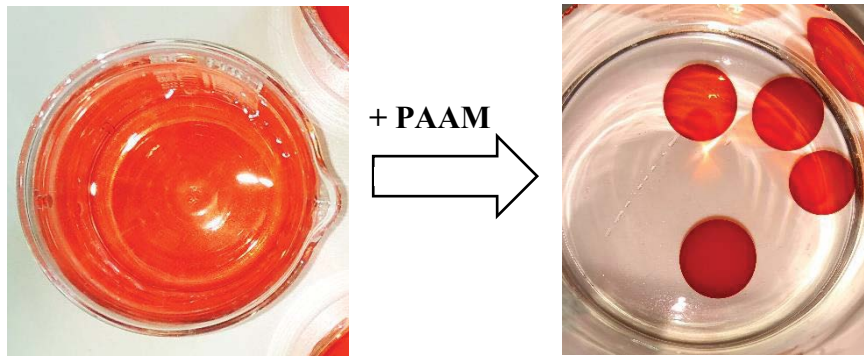


Fig. 4. Safranin dye adsorption on PAAM hydrogel.

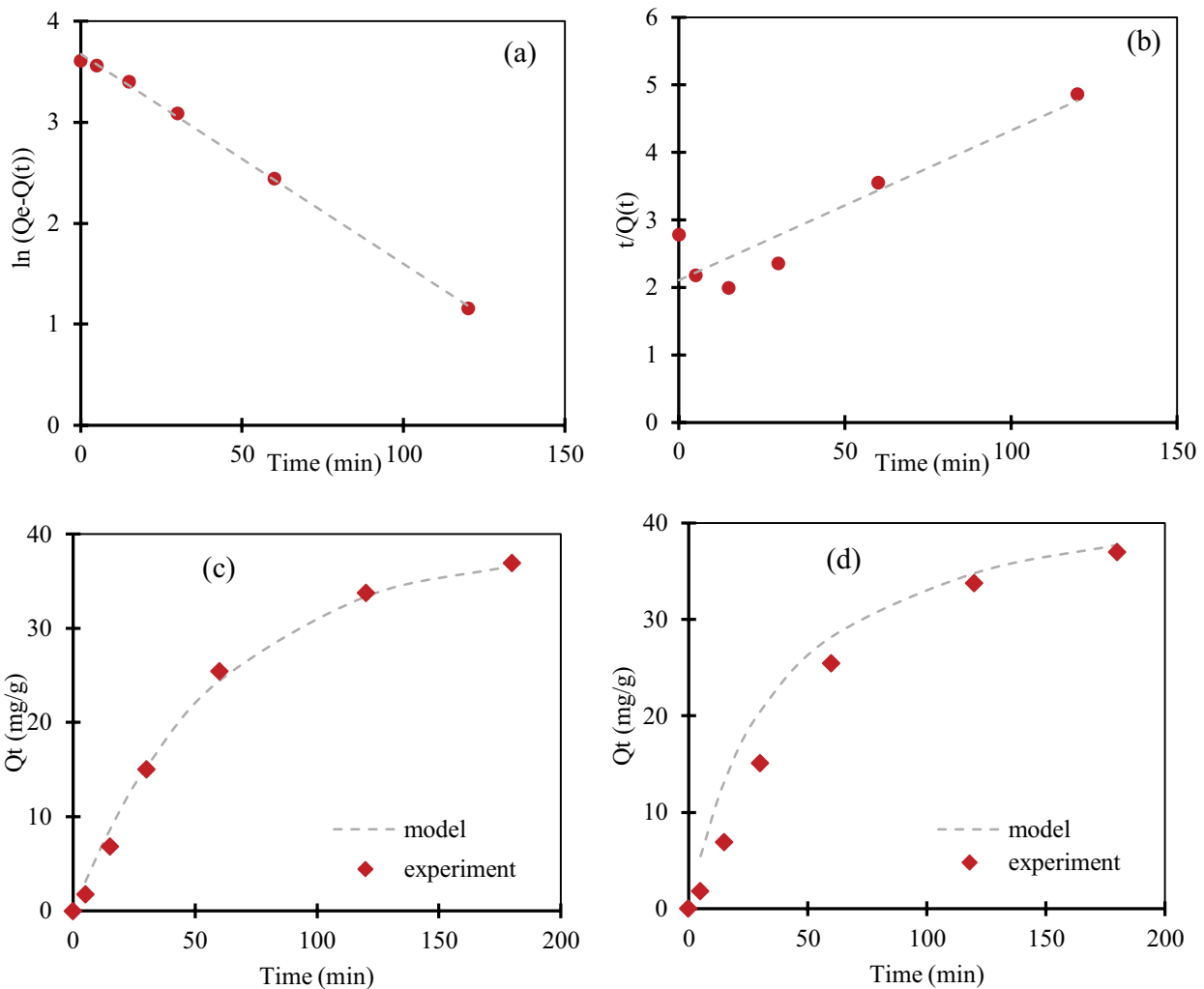


Fig. 5. Linear pseudo-first-order (a), linear pseudo-second-order (b), nonlinear pseudo-first-order (c), and nonlinear pseudo-second-order (d) kinetic studies of SF adsorption on PAAM.

were determined at different temperatures with an initial dye concentration of 10 mg/L (Fig. 6). Table 5 gives the values for standard free enthalpy, standard enthalpy, and standard entropy. It can be deduced from the table that the positive value of  $\Delta H$  confirms the endothermic nature

of the adsorption of SF on PAAM. The negative value of  $\Delta G$  reveals the spontaneity of the adsorption process. The positive value of  $\Delta S$  demonstrates randomness at the solid-solute interface. Those results are similar to the ones found by Jawad et al. [60].

Table 3  
Kinetic constants of the pseudo-first and second-order models

$Q_{\max, \text{exp}} = 36.97$	Pseudo-first-order model		Pseudo-second-order model	
	$Q_1$ (mg/g)	$K_1$ ( $\text{min}^{-1}$ )	$Q_2$ (mg/g)	$K_2 \cdot 10^{-4}$ (g/mg min)
Linear	39.36	0.0208	45.04	2.33
Non linear	38.49	0.016	45.43	6.2

Table 4  
Kinetic error deviation related to the adsorption of SF dye onto PAAM

	$R^2$	$\chi^2$	SSE	SE	F-ratio
Linear					
Pseudo-first-order	0.96	3.53	47.13	2.80	1.08
Pseudo-second-order	0.81	11.22	238.30	6.30	1.55
Nonlinear					
Pseudo-first-order	0.99	0.94	6.55	1.04	1.05
Pseudo-second-order	0.92	7.35	97.18	4.02	1.26

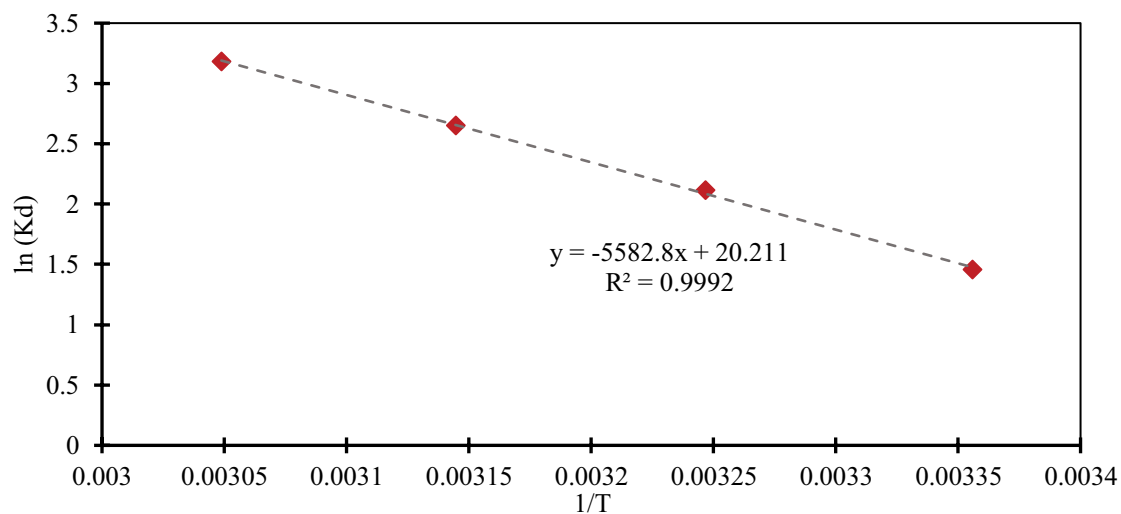


Fig. 6. Van't Hoff curve of SF adsorption on PAAM.

Table 5  
Thermodynamic parameters of SF adsorption on PAAM

$T$ (K)	$\Delta H$ (KJ/mol)	$\Delta S$ (J/mol K)	$\Delta G$ (J/mol)	$R^2$
298	46.41	168.03	-3,535.58	0.9992
308			-5,298.61	
318			-6,857.01	
328			-8,490.27	

### 3.5.1. Effect of the concentration

To study the effect of the initial concentration of the SF dye on the adsorption capacity of the PAAM gel, the procedure was performed with an initial dye concentration

that varies between 10 and 600 mg/L for 180 min, while maintaining constant the other parameters (Fig. 3d). It can be observed from the curve that the adsorption capacity of PAAM increases with increasing SF dye concentration. Beyond a concentration of 280 mg/L, an equilibrium is observed due to the saturation of the active sites of the adsorbent in the presence of a high dye content. In fact, the increase in concentration induces an increase in the driving force of the concentration gradient, thus increasing the diffusion of the dye molecules in solution through the surface of the adsorbent [61]. The maximum load of PAAM in SF expressed in mg of fixed dye per g of PAAM polymer is 620 mg/g. Similar results were found by Rajabi et al. [62].

3.6. Adsorption isotherm

The experimental data of SF dye binding to polyacrylamide are processed according to the linear and nonlinear regression of Langmuir and Freundlich (Fig. 7). This modulization aims to be able to verify the model according to which the adsorption takes place and to deduce from it the maximum adsorbed quantities as well as the affinity of the adsorbate for the adsorbent [63]. The Langmuir isotherm assumes that monolayer adsorption occurs at binding sites with homogenous energy levels, no

interactions between adsorbed molecules, and no transmigration of adsorbed molecules on the adsorption surface [64]. The Freundlich isotherm is an empirical equation that assumes a heterogeneous adsorbent surface with its adsorption sites at varying energy levels [65]. Table 6 gathers the values of Freundlich and Langmuir constants, extrapolated from the linear curves of the models.

By comparing the  $R^2$ ,  $\chi^2$ , SE, and SSE values from Table 7, the sorption isotherm models fitted the experimental data in the order Langmuir > Freundlich. The experimental data were best described by the Langmuir

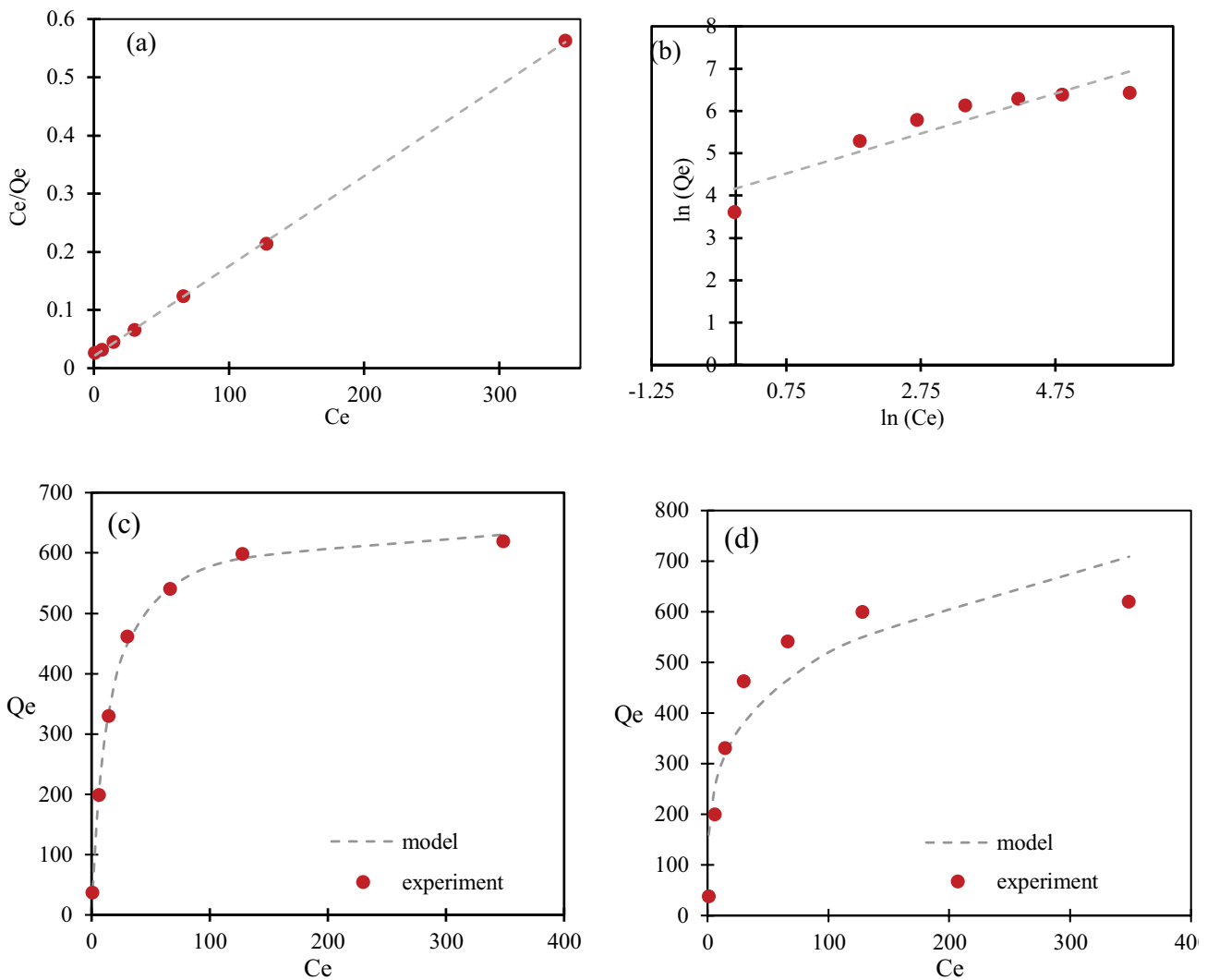


Fig. 7. Adsorption isotherm modeling of SF dye removal using PAAM with linear regression ((a) Langmuir and (b) Freundlich) and nonlinear regression ((c) Langmuir and (d) Freundlich).

Table 6  
Freundlich and Langmuir adsorption parameters of SF dye on PAAM.

$Q_{\max, \text{exp}}$ (mg/g) = 620.9	Freundlich model		Langmuir model		
	$1/n$	$K_f$ (mg/g)(L/mg) $^{1/n}$	$Q_{\max}$ (mg/g)	$K_L$ (L/mg)	$R_L$
Linear	0.472	64.59	666.66	0.072	0.568–0.0266
Non linear	0.253	160.48	655.64	0.071	0.584–0.0273

isotherm model by providing the highest  $R^2$  and the lowest  $\chi^2$ , SE, and SSE values. Also, the maximum adsorbed quantity obtained by the Langmuir model is very close to that obtained experimentally. These results indicate that the adsorption of SF dye to PAAM follows Langmuir's model for both linear and non-linear analysis. In addition, the Hall constant  $R_L < 1$  implying that the adsorption of SF on PAAM is favorable [31]. On the other hand, the  $R^2$ ,  $\chi^2$ , SE and SSE values show that the best-fitting isotherm model is the non-linear regression approach, indeed this method avoids errors, making this analyzing technique the most appropriate to obtain more realistic isotherm parameters. Langmuir is a commonly used model for describing this single-layer adsorption mechanism. Assuming that all the adsorption sites are equivalent and that the adsorption layer is unimolecular in thickness, the resulting adsorbent surface has a limited number of adsorption sites and only one molecule can be occupied at each site [66]. Similar results have also been reported by other researchers as well in the adsorption of SF dye [67,68].

### 3.6.1. Mechanism of SF dye adsorption

To demonstrate the suggested mechanism of SF dye adsorption on PAAM, Fourier-transform infrared

Table 7  
Isotherm error deviation related to the adsorption of SF dye onto PAAM

	$R^2$	$\chi^2$	SSE	SE	F-ratio
Linear					
Langmuir	0.996	2.93	892.56	12.19	1.023
Freundlich	0.300	301.35	202,085.65	183.52	1.55
Nonlinear					
Langmuir	0.998	1.78	463.33	8.78	0.99
Freundlich	0.858	152.23	40,971.96	82.63	1.39

spectroscopy of PAAM before and after dye adsorption, were measured and compared (Fig. 8). After dye adsorption, positions, and intensities of characteristic functional groups such as C–H and C–N stretching bands (2,923 and 1,382  $\text{cm}^{-1}$ ), was unchanged. These results suggested that these functional groups on the surface of PAAM do not participate in the whole adsorption process. However, the N–H and C=O stretching vibration bands at 3,465.44; 622 and 1,382  $\text{cm}^{-1}$  showed an important variation in the intensity further confirming that those two functional groups available on surface PAAM hydrogel that can be involved in the adsorption mechanism of SF dye. The adsorption mechanism of SF onto PAAM composite can be attributed to different types of interactions as shown in Fig. 9. Electrostatic attractions can be considered as the most impactful attraction force that can be occurred between SF dye and PAAM surface. This mechanism involves the electrostatic interaction between negatively charged groups of dye with an amino group ( $-\text{NH}_2$ ) and (=O) group positively charged available on the adsorbent surface. The adsorption mechanism also includes hydrogen bonding and n–n interaction.

For comparative purposes, the maximum adsorption capacities of some adsorbents, based on polyacrylamide, reported previously for the removal of dyes are summarized in Table 8. The results show that the PAAM hydrogel is a suitable adsorbent for cationic dye removal.

## 4. Conclusion

We investigated in this study, the swelling behavior of polyacrylamide hydrogel in distilled water and its capacity to adsorb SF dye, by varying physicochemical parameters. It was found that the swelling of the hydrogel and its adsorption capacity were affected by different parameters. The maximum swelling rate of PAAM hydrogel is 100. The maximum amount of SF dye adsorbed by PAAM is 620.9 mg/g. The optimum pH for the adsorption process was 4–8. Kinetic studies showed that the adsorption of SF dye on PAAM reached equilibrium in 180 min. The

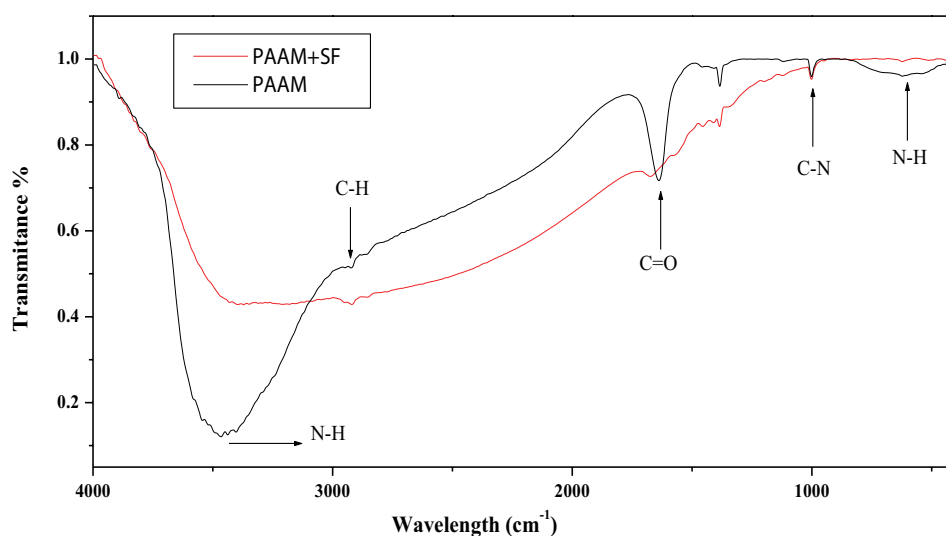


Fig. 8. Fourier-transform infrared spectroscopy of PAAM before and after SF dye adsorption.

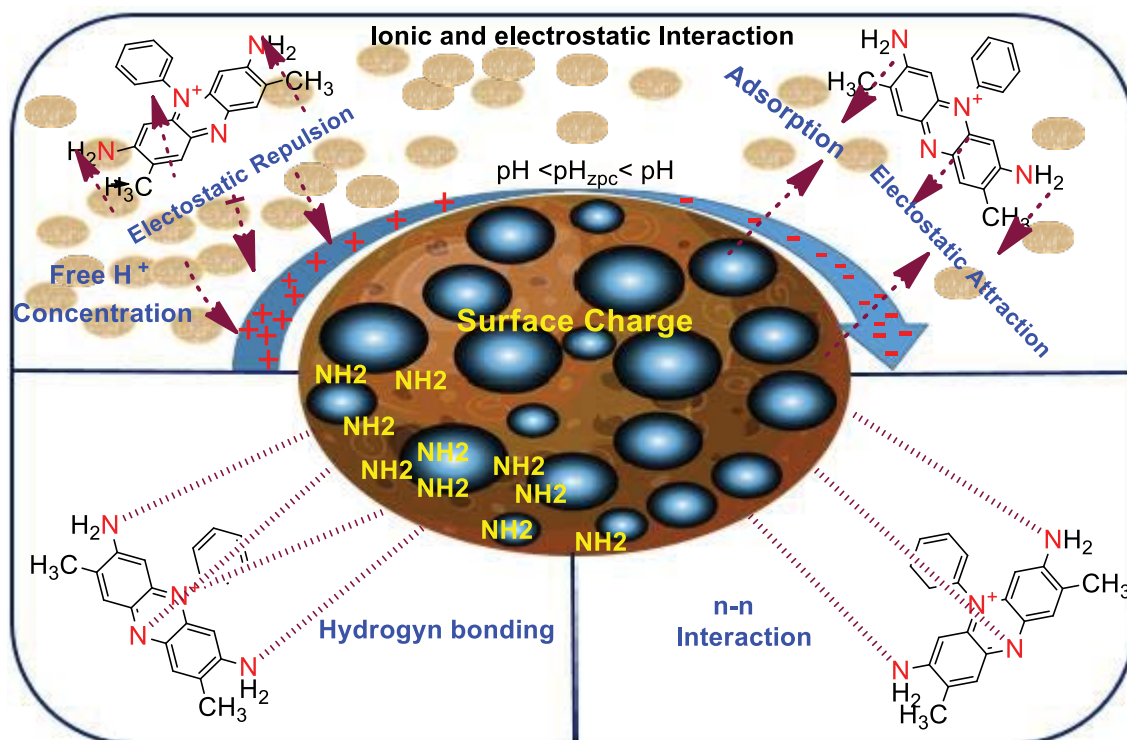


Fig. 9. Possible interactions contributing to the mechanism of SF adsorption on PAAM.

Table 8

Comparison of maximum adsorption capacity of dyes onto different adsorbent based on polyacrylamide

Adsorbent	$Q_m$ (mg/g)	References
Polyacrylamide/polyacrylate/gum Arabic	48	[69]
Amphoteric grafting flocculant carboxymethyl chitosan-graft-polyacrylamide	70	[39]
Porous Carrageenan-g-polyacrylamide/bentonite	156.25	[70]
Hydrolyzed polyacrylamide/cellulose nanocrystal	326.08	[38]
Polyacrylamide	620.9	The present study
Porous magnetic polyacrylamide microspheres	1,990	[71]

endothermic and spontaneous natures of SF adsorption on PAAM were also observed. This suggested utilization of higher temperatures for favorable and high performance of SF adsorption.

The related results have been modeled using Freundlich, Langmuir, pseudo-first-order, and pseudo-second-order equations, via both linear and non-linear regression analysis. The best-fitting model was evaluated using five different statistical tools ( $R^2$ ,  $\chi^2$ , SEE, SE, and  $F$ -test). The examination of all these error estimation methods showed that the Langmuir model and the pseudo-first-order provide the best fit for the experimental equilibrium and kinetic data, respectively (i.e. highest  $R^2$  and lowest  $\chi^2$ , SEE, SE,  $F$ -value). On the other hand, nonlinear regression analysis seems to be adequate to point out the best-fitting model.

Although an increasing number of studies included hydrogel and its application for dyes adsorption, there are still several points that need more attention, such as improvement of adsorption capacity by modification of adsorbent,

treatment of multicomponent mixtures of dyes, adsorption application for real industrial effluents, and regeneration studies. Furthermore, studies should also be extended to pilot and full scale to evaluate the potential use of PAAM hydrogel at the industrial level.

#### Acknowledgements

We gratefully acknowledge the Technical Support Units for Scientific Research (UATRS) under the National Center for Scientific and Technical Research (CNRST), especially to Hanae OUAADARI for the analytical services and instrumentations. We also thank our laboratory members for their generous help.

#### References

- [1] H. Daud, A. Ghani, D.N. Iqbal, N. Ahmad, S. Nazir, M.J. Muhammad, E.A. Hussain, A. Nazir, M. Iqbal, Preparation

- and characterization of guar gum based biopolymeric hydrogels for controlled release of antihypertensive drug, *Arabian J. Chem.*, 14 (2021) 103111, doi: 10.1016/j.arabjc.2021.103111.
- [2] D.N. Iqbal, S. Shafiq, S.M. Khan, S.M. Ibrahim, S.A. Abubshait, A. Nazir, M. Abbas, M. Iqbal, Novel chitosan/guar gum/PVA hydrogel: preparation, characterization and antimicrobial activity evaluation, *Int. J. Biol. Macromol.*, 164 (2020) 499–509.
  - [3] X. Wang, H. Hou, Y. Li, Y. Wang, C. Hao, A novel semi-IPN hydrogel: preparation, swelling properties and adsorption studies of Co(II), *J. Ind. Eng. Chem.*, 41 (2016) 82–90.
  - [4] F.N. Muya, C.E. Sunday, P. Baker, E. Iwuoha, Environmental remediation of heavy metal ions from aqueous solution through hydrogel adsorption: a critical review, *Water Sci. Technol.*, 73 (2016) 983–992.
  - [5] A. Ouass, Y. Essaadaoui, L. Kadiri, I. Lebkiri, C. Lafreme, M. Cherkaoui, A. Lebkiri, E.H. Rifi, Adsorption of Cr(III) from aqueous solution by two forms of a superabsorbant polymer: parametric study and effect of activation mode, *E3S Web Conf.*, 37 (2018) 02001, doi: 10.1051/e3sconf/20183702001.
  - [6] T. Wells Jr., M. Kosa, A. Ragauskas, Polymerization of Kraft lignin via ultrasonication for high-molecular-weight applications, *Ultrason. Sonochem.*, 20 (2013) 1463–1469.
  - [7] Y.H. Teow, L.M. Kam, A.W. Mohammad, Synthesis of cellulose hydrogel for copper(II) ions adsorption, *J. Environ. Chem. Eng.*, 6 (2018) 4588–4597.
  - [8] A. Asfaram, M. Ghaedi, S. Hajati, M. Rezaeinejad, A. Goudarzi, M. Purkait, Rapid removal of Auramine-O and Methylene blue by ZnS:Cu nanoparticles loaded on activated carbon: a response surface methodology approach, *J. Taiwan Inst. Chem. Eng.*, 53 (2015) 80–91.
  - [9] E. Dil, M. Ghaedi, A. Asfaram, F. Mehrabi, A. Bazrafshan, A. Ghaedi, Trace determination of safranin O dye using ultrasound assisted dispersive solid-phase micro extraction: artificial neural network-genetic algorithm and response surface methodology, *Ultrason. Sonochem.*, 33 (2016) 129–140.
  - [10] J. Luan, P.-X. Hou, C. Liu, C. Shi, G.-X. Li, H.-M. Cheng, Efficient adsorption of organic dyes on a flexible single-wall carbon nanotube film, *J. Mater. Chem. A*, 4 (2016) 1191–1194.
  - [11] M. Iqbal, *Vicia faba* bioassay for environmental toxicity monitoring: a review, *Chemosphere*, 144 (2016) 785–802.
  - [12] S. Chandra, L.K.S. Chauhan, P.N. Pande, S.K. Gupta, Cytogenetic effects of leachates from tannery solid waste on the somatic cells of *Vicia faba*, *Environ. Toxicol.*, 19 (2004) 129–133.
  - [13] M. Gaddekar, A. Ahammed, Modelling dye removal by adsorption onto water treatment residuals using combined response surface methodology-artificial neural network approach, *J. Environ. Manage.*, 231 (2019) 241–248.
  - [14] S. Homaeigohar, The nanosized dye adsorbents for water treatment, *Nanomaterials*, 10 (2020) 295, doi: 10.3390/nano10020295.
  - [15] I. Anastopoulos, A. Hosseini-Bandegharai, J. Fu, A.C. Mitropoulos, G.Z. Kyzas, Use of nanoparticles for dye adsorption: review, *J. Dispersion Sci. Technol.*, 39 (2018) 836–847.
  - [16] Z. Huang, Y. Li, W. Chen, J. Shi, N. Zhang, Z. Wang, Y. Zhang, Modified bentonite adsorption of organic pollutants of dye wastewater, *Mater. Chem. Phys.*, 202 (2017) 266–276.
  - [17] I. Lebkiri, B. Abbou, L. Kadiri, A. Ouass, Y. Essaadaoui, A. Habssaoui, E.H. Rifi, A. Lebkiri, Removal of methylene blue dye from aqueous solution using a superabsorbant hydrogel the polyacrylamide: isotherms and kinetic studies, *Mediter. J. Chem.*, 9 (2019) 337–346.
  - [18] X. Zou, H. Zhang, T. Chen, H. Li, C. Meng, Y. Xia, J. Guo, Preparation and characterization of polyacrylamide/sodium alginate microspheres and its adsorption of MB dye, *Colloids Surf., A*, 567 (2019) 184–192.
  - [19] T. Bertrand, J. Peixinho, S. Mukhopadhyay, C.W. MacMinn, Dynamics of swelling and drying in a spherical gel, *Phys. Rev. Appl.*, 6 (2016) 064010, doi: 10.1103/PhysRevApplied.6.064010.
  - [20] K. Moreno-Sader, A. Garcia-Padilla, A. Realpe, M. Acevedo-Morantes, J.B.P. Soares, Removal of heavy metal water pollutants (Co<sup>2+</sup> and Ni<sup>2+</sup>) using polyacrylamide/sodium montmorillonite (PAM/Na-MMT) nanocomposites, *ACS Omega*, 4 (2019) 10834–10844.
  - [21] M. Wiśniewska, G. Fijałkowska, K. Szewczuk-Karpisz, The mechanism of anionic polyacrylamide adsorption on the montmorillonite surface in the presence of Cr(VI) ions, *Chemosphere*, 211 (2018) 524–534.
  - [22] J. Rahchamani, H.Z. Mousavi, M. Behzad, Adsorption of methyl violet from aqueous solution by polyacrylamide as an adsorbent: isotherm and kinetic studies, *Desalination*, 267 (2011) 256–260.
  - [23] K. Didehban, M. Hayasi, F. Kermajani, Removal of anionic dyes from aqueous solutions using polyacrylamide and polyacrylic acid hydrogels, *Korean J. Chem. Eng.*, 34 (2017) 1177–1186.
  - [24] H. Mousavi, A. Khaligh, M. Behzad, J. Rahchamani, Application of polyacrylamide for methylene blue removal from aqueous solutions, *J. Appl. Solution Chem. Model.*, 3 (2014) 39–47.
  - [25] B. Abbou, I. Lebkiri, H. Ouaddari, O. Elkhatabi, A. Habssaoui, A. Lebkiri, E.H. Rifi, Kinetic and thermodynamic study on adsorption of cadmium from aqueous solutions using natural clay, *J. Turk. Chem. Soc. Sect. Chem.*, 8 (2021) 677–692.
  - [26] L. Kadiri, A. Lebkiri, E.H. Rifi, A. Ouass, Y. Essaadaoui, I. Lebkiri, H. Hamad, Kinetic studies of adsorption of Cu (II) from aqueous solution by coriander seeds (*Coriandrum Sativum*), *E3S Web Conf.*, 37 (2018) 02005, doi: 10.1051/e3sconf/20183702005.
  - [27] N.P. Shetti, S.J. Malode, R.S. Malladi, S.L. Nargund, S.S. Shukla, T.M. Aminabhavi, Electrochemical detection and degradation of textile dye Congo red at graphene oxide modified electrode, *Microchem. J.*, 146 (2019) 387–392.
  - [28] I. Sohail, I.A. Bhatti, A. Ashar, F.M. Sarim, M. Mohsin, R. Naveed, M. Yasir, M. Iqbal, A. Nazir, Polyamidoamine (PAMAM) dendrimers synthesis, characterization and adsorptive removal of nickel ions from aqueous solution, *J. Mater. Res. Technol.*, 9 (2020) 498–506.
  - [29] R. Naveed, I.A. Bhatti, I. Sohail, A. Ashar, S.M. Ibrahim, M. Iqbal, A. Nazir, Kinetic and equilibrium study of (poly amido amine) PAMAM dendrimers for the removal of chromium from tannery wastewater, *Z. Für Phys. Chem.*, 1 (2020), doi: 10.1515/zpch-2019-1567 (in Press).
  - [30] C.S.T. Araújo, I.L.S. Almeida, H.C. Rezende, S.M.L.O. Marcionilio, J.J.L. Léon, T.N. de Matos, Elucidation of mechanism involved in adsorption of Pb(II) onto lobeira fruit (*Solanum lycocarpum*) using Langmuir, Freundlich and Temkin isotherms, *Microchem. J.*, 137 (2018) 348–354.
  - [31] A. Ouass, I. Ismi, H. Elaidi, A. Lebkiri, M. Cherkaoui, E.H. Rifi, Mathematical modeling of the adsorption of trivalent chromium by the sodium polyacrylate beads, *J. Mater. Environ. Sci.*, 8 (2017) 3448–3456.
  - [32] Y. Essaadaoui, A. Lebkiri, E. Rifi, L. Kadiri, A. Ouass, Adsorption of lead by modified *Eucalyptus camaldulensis* barks: equilibrium, kinetic and thermodynamic studies, *Desal. Water Treat.*, 111 (2018) 267–277.
  - [33] A. Chakir, J. Bessiere, K.E. Kacemi, B. Marouf, A comparative study of the removal of trivalent chromium from aqueous solutions by bentonite and expanded perlite, *J. Hazard. Mater.*, 95 (2002) 29–46.
  - [34] N.P. Raval, M. Kumar, Geogenic arsenic removal through core-shell based functionalized nanoparticles: groundwater in-situ treatment perspective in the post-COVID anthropocene, *J. Hazard. Mater.*, 402 (2021) 123466, doi: 10.1016/j.jhazmat.2020.123466.
  - [35] J. Sreńscek-Nazzal, U. Narkiewicz, A.W. Morawski, R.J. Wróbel, B. Michalkiewicz, Comparison of optimized isotherm models and error functions for carbon dioxide adsorption on activated carbon, *J. Chem. Eng. Data*, 60 (2015) 3148–3158.
  - [36] N. Yuan, L. Xu, L. Zhang, H. Ye, J. Zhao, Z. Liu, J. Rong, Superior hybrid hydrogels of polyacrylamide enhanced by bacterial cellulose nanofiber clusters, *Mater. Sci. Eng. C*, 67 (2016) 221–230.
  - [37] R. Liu, S. Liang, X.-Z. Tang, D. Yan, X. Li, Z.-Z. Yu, Tough and highly stretchable graphene oxide/polyacrylamide

- nanocomposite hydrogels, *J. Mater. Chem.*, 22 (2012) 14160–14167.
- [38] C. Zhou, Q. Wu, T. Lei, I.I. Negulescu, Adsorption kinetic and equilibrium studies for methylene blue dye by partially hydrolyzed polyacrylamide/cellulose nanocrystal nanocomposite hydrogels, *Chem. Eng. J.*, 251 (2014) 17–24.
- [39] Z. Yang, H. Yang, Z. Jiang, T. Cai, H. Li, H. Li, A. Li, R. Cheng, Flocculation of both anionic and cationic dyes in aqueous solutions by the amphoteric grafting flocculant carboxymethyl chitosan-graft-polyacrylamide, *J. Hazard. Mater.*, 254–255 (2013) 36–45.
- [40] X. Wei, J. Tao, M. Li, B. Zhu, X. Li, Z. Ma, T. Zhao, B. Wang, B. Suo, H. Wang, J. Yang, L. Ye, X. Qi, Polyacrylamide-based inorganic hybrid flocculants with self-degradable property, *Mater. Chem. Phys.*, 192 (2017) 72–77.
- [41] F. Yang, G. Li, Y.-G. He, F.-X. Ren, G. Wang, Synthesis, characterization, and applied properties of carboxymethyl cellulose and polyacrylamide graft copolymer, *Carbohydr. Polym.*, 78 (2009) 95–99.
- [42] R.I. Baron, M. Bercea, M. Avadanei, G. Lisa, G. Biliuta, S. Coseri, Green route for the fabrication of self-healable hydrogels based on tricarboxy cellulose and poly(vinyl alcohol), *Int. J. Biol. Macromol.*, 123 (2019) 744–751.
- [43] H.T. Nguyen, V.N. Phuong, T.N. Van, P.N. Thi, P. Dinh Thi Lan, H.T. Pham, H.T. Cao, Low-cost hydrogel derived from agro-waste for veterinary antibiotic removal: optimization, kinetics, and toxicity evaluation, *Environ. Technol. Innovation*, 20 (2020) 101098, doi: 10.1016/j.eti.2020.101098.
- [44] R. Bhadani, U.K. Mitra, Synthesis and studies on water swelling behaviour of polyacrylamide hydrogels, *Macromol. Symp.*, 369 (2016) 30–34.
- [45] D. Saraydın, E. Karadağ, Y. Işıkver, N. Şahiner, O. Güven, The influence of preparation methods on the swelling and network properties of acrylamide hydrogels with crosslinkers, *J. Macromol. Sci. Part A*, 41 (2004) 419–431.
- [46] T. Begam, A.K. Nagpal, R. Singhal, A comparative study of swelling properties of hydrogels based on poly(acrylamide-co-methyl methacrylate) containing physical and chemical crosslinks, *J. Appl. Polym. Sci.*, 89 (2003) 779–786.
- [47] G.R. Mahdavinia, A. Pourjavadi, H. Hosseinzadeh, M.J. Zohuriaan, Modified chitosan 4 superabsorbent hydrogels from poly(acrylic acid-co-acrylamide) grafted chitosan with salt- and pH-responsiveness properties, *Eur. Polym. J.*, 40 (2004) 1399–1407.
- [48] S. Ata, A. Rasool, A. Islam, I. Bibi, M. Rizwan, M.K. Azeem, A. ur R. Qureshi, M. Iqbal, Loading of Cefixime to pH sensitive chitosan based hydrogel and investigation of controlled release kinetics, *Int. J. Biol. Macromol.*, 155 (2020) 1236–1244.
- [49] P.C. Parvathy, A.N. Jyothi, Synthesis, characterization and swelling behaviour of superabsorbent polymers from cassava starch-graft-poly(acrylamide), *Starch-Stärke*, 64 (2012) 207–218.
- [50] T. Jayaramudu, H.-U. Ko, H.C. Kim, J.W. Kim, J. Kim, Swelling behavior of polyacrylamide–cellulose nanocrystal hydrogels: swelling kinetics, temperature, and pH effects, *Materials*, 12 (2019) 2080, doi: 10.3390/ma12132080.
- [51] B. Abbou, I. Lebkiri, H. Ouaddari, L. Kadiri, A. Ouass, A. Habsaoui, A. Lebkiri, E.H. Rifi, Removal of Cd(II), Cu(II), and Pb(II) by adsorption onto natural clay: a kinetic and thermodynamic study, *Turk. J. Chem.*, 45 (2021) 362–376.
- [52] H. Moussout, H. Ahlafi, M. Aazza, H. Maghat, Critical of linear and nonlinear equations of pseudo-first order and pseudo-second order kinetic models, *Karbala Int. J. Mod. Sci.*, 4 (2018) 244–254.
- [53] R. Liu, B. Zhang, D. Mei, H. Zhang, J. Liu, Adsorption of methyl violet from aqueous solution by halloysite nanotubes, *Desalination*, 268 (2011) 111–116.
- [54] G. Sara, A. Mahdad-Benzerdjeb, M. Ameri, A.Z. Bouyakoub, Adsorption of 2,4,6-trichlorophenol on bentonite modified with benzylidimethyltetradecylammonium chloride, *Chem. Int.*, 4 (2019) 24–32.
- [55] M. Boutayeb, A. Bouzidi, M. Fekhaoui, Etude de la qualité physico-chimique des eaux usées brutes de cinq villes de la région de la Chaouia–Ouardigha (Maroc), *Bull. L'institut Sci. Rabat Sect. Sci. Vie*, 34 (2012) 145–150.
- [56] Y. Essaadaoui, A. Lebkiri, E.H. Rifi, L. Kadiri, A. Ouass, Adsorption of cobalt from aqueous solutions onto Bark of Eucalyptus, *Mediterr. J. Chem.*, 7 (2018) 145–155.
- [57] R. Wei, W. Song, F. Yang, J. Zhou, M. Zhang, X. Zhang, W. Zhao, C. Zhao, Bidirectionally pH-responsive Zwitterionic polymer hydrogels with switchable selective adsorption capacities for anionic and cationic dyes, *Ind. Eng. Chem. Res.*, 57 (2018) 8209–8219.
- [58] M. Constantin, I. Asmarandei, V. Harabagiu, L. Ghimici, P. Ascenzi, G. Fundueanu, Removal of anionic dyes from aqueous solutions by an ion-exchanger based on pullulan microspheres, *Carbohydr. Polym.*, 91 (2013) 74–84.
- [59] L. Liu, Z.Y. Gao, X.P. Su, X. Chen, L. Jiang, J.M. Yao, Adsorption removal of dyes from single and binary solutions using a cellulose-based bioadsorbent, *ACS Sustainable Chem. Eng.*, 3 (2015) 432–442.
- [60] A.H. Jawad, N.S.A. Mubarak, A.S. Abdulhameed, Hybrid crosslinked Chitosan-Epichlorohydrin/TiO<sub>2</sub> nanocomposite for Reactive Red 120 dye adsorption: kinetic, isotherm, thermodynamic, and mechanism study, *J. Polym. Environ.*, 28 (2020) 624–637.
- [61] F. Deniz, S.D. Saygideger, Investigation of adsorption characteristics of Basic Red 46 onto gypsum: equilibrium, kinetic and thermodynamic studies, *Desalination*, 262 (2010) 161–165.
- [62] M. Rajabi, K. Mahanpoor, O. Moradi, Preparation of PMMA/GO and PMMA/GO-Fe<sub>3</sub>O<sub>4</sub> nanocomposites for malachite green dye adsorption: kinetic and thermodynamic studies, *Compos. Part B Eng.*, 167 (2019) 544–555.
- [63] L. Li, L. Fan, H. Duan, X. Wang, C. Luo, Magnetically separable functionalized graphene oxide decorated with magnetic cyclodextrin as an excellent adsorbent for dye removal, *RSC Adv.*, 4 (2014) 37114–37121.
- [64] M. Hanafiah, W. Ngah, S. Zolkafly, L. Teong, Z. Majid, Acid Blue 25 adsorption on base treated *Shorea dasyphylla* sawdust: kinetic, isotherm, thermodynamic and spectroscopic analysis, *J. Environ. Sci.*, 24 (2012) 261–268.
- [65] H. Freundlich, Über die Adsorption in Lösungen, *Z. Für Phys. Chem.*, 57U (1907) 385–470.
- [66] X.X. Liang, A.M. Omer, Z. Hu, Y. Wang, D. Yu, X. Ouyang, Efficient adsorption of diclofenac sodium from aqueous solutions using magnetic amine-functionalized chitosan, *Chemosphere*, 217 (2019) 270–278.
- [67] S. Kaur, S. Rani, R.K. Mahajan, M. Asif, V.K. Gupta, Synthesis and adsorption properties of mesoporous material for the removal of dye safranin: kinetics, equilibrium, and thermodynamics, *J. Ind. Eng. Chem.*, 22 (2015) 19–27.
- [68] M.R. Abukhadra, A.S. Mohamed, Adsorption removal of Safranin Dye contaminants from water using various types of natural zeolite, *Silicon*, 11 (2019) 1635–1647.
- [69] A.T. Paulino, M.R. Guilherme, A.V. Reis, G.M. Campese, E.C. Muniz, J. Nozaki, Removal of methylene blue dye from an aqueous media using superabsorbent hydrogel supported on modified polysaccharide, *J. Colloid Interface Sci.*, 301 (2006) 55–62.
- [70] A. Pourjavadi, Z. Bassampour, H. Ghasemzadeh, M. Nazari, L. Zolghadr, S.H. Hosseini, Porous Carrageenan-g-polyacrylamide/bentonite superabsorbent composites: swelling and dye adsorption behavior, *J. Polym. Res.*, 23 (2016) 60, doi: 10.1007/s10965-016-0955-z.
- [71] T. Yao, S. Guo, C. Zeng, C. Wang, L. Zhang, Investigation on efficient adsorption of cationic dyes on porous magnetic polyacrylamide microspheres, *J. Hazard. Mater.*, 292 (2015) 90–97.

## Supplementary information

